Energy Conversion and Management 246 (2021) 114672

Contents lists available at ScienceDirect

Energy Conversion and Management

journal homepage: www.elsevier.com/locate/enconman

Different design aspects of an Organic Rankine Cycle turbine for electricity production using a geothermal binary power plant

Paweł Ziółkowski [a,*], Rafał Hyrzyński [b], Marcin Lemański [b], Bartosz Kraszewski [b], Sebastian Bykuć [b], Stanisław Głuch [a], Anna Sowiżdżał [c], Leszek Pająk [c], Anna Wachowicz-Pyzik [c], Janusz Badur [b]

[a] Gdańsk University of Technology, Faculty of Mechanical Engineering and Shipbuilding, Energy Institute Narutowicza 11/12, 80-233 Gdańsk, Poland
[b] Institute of Fluid Flow Machinery, Polish Academy of Science, Fiszera 14, 80-231 Gdańsk, Poland
[c] AGH University of Science and Technology, Faculty of Geology, Geophysics and Environmental Protection, Department of Fossil Fuels, Poland

ARTICLE INFO

Keyword:
Axial turbine
Binary power plant
Geothermal energy
Renewable energy
Thermodynamic analysis
Turbine design

ABSTRACT

In recent years, pressure has been growing to increase the share of renewable energy sources in electricity generation, which may offer opportunities for the development of geothermal energy in regions that have been so far considered unprofitable in this respect. One such country currently undergoing an energy transition is Poland in which low-temperature geothermal resources are currently used for district heating and recreation purposes. Nevertheless, research on the possibilities of using geothermal energy for electricity production is ongoing. The objective of this paper was to perform a comprehensive analysis of a binary power plant construction in relation to low-temperature petro-geothermal resources. The potential binary power plant is located in the area characterized by temperature of 120 °C at depths of 5000 m. About half of Poland's area, especially the regions of western and central Poland, has these characteristics. It was assumed that brine at volume flow rate of 400 m^3/h is a heat source for the Organic Rankine Cycle with isobutane as a working medium. The thermal efficiency based on the First Law of Thermodynamics and the power output were estimated at 10.5% and 1.79 MW_e, respectively. In addition, the thermal efficiency based on the Second Law of Thermodynamics was calculated at 29.0%. For the calculated cycle parameters, a preliminary design of a two-stage axial turbine was constructed. All results were compared to the other binary power plants and they confirm that establishing the binary power plant in Poland would be thermodynamically justified. The main novelty of the present work is the combination of three issues, namely the selection of the low- temperature heat source, the design and analysis of the cycle together with a turbine adapted to these conditions.

1. Introduction

In the recent years, the global climate change, ozone layer destruction, growth of electrical energy consumption and reduction of fossil fuel sources have become factors in the improvement of renewable energy sources (RES) technology. Wind and photovoltaic farms are relatively popular presently, but it should be noted that their operation is dependent on weather conditions [1]. Thus, due to the significant unpredictability of the supplied power, they require cooperation with conventional power plants [2] and energy storage technologies that are also being developed with consideration of caverns [3] or fuel cell technology [4]. On the other hand, biomass combustion technologies and both, hydroelectric and geothermal power plants can be classified as relatively stable or at least as cyclical RES [5]. However, biomass power plants, despite the possibility of compact construction, require large amounts of low-energy feedstocks, usually sourced from large areas of land; the exception to this prosses is waste management [6]. Hydroelectric power plants, on the other hand, are usually characterised by high contamination of the local water environment [3]. Geothermal power plants are distinguished by their small-scale surface impact on the local environment in which energy in the form of heat is extracted by drilling vertically, deep into the ground [7]. The European Union's (EU) 2014 regulations for a minimum share of 27% of electricity generated from RES [8] have contributed to the dynamic development of RES technologies. Thus it is an opportunity for the development of

* Corresponding author.
E-mail addresses: pawel.ziolkowski1@pg.edu.pl (P. Ziółkowski), ansow@agh.edu.pl (A. Sowiżdżał), pajakl@agh.edu.pl (L. Pająk), amwachow@agh.edu.pl (A. Wachowicz-Pyzik).

https://doi.org/10.1016/j.enconman.2021.114672
Received 23 February 2021; Accepted 18 August 2021
Available online 2 September 2021

Nomenclature

a	velocity of sound propagation, m/s
c	specific heat, J/(kg K); turbine stage absolute velocity, m/s
d_{av}	average diameter of the blade row, m
e	specific exergy, J/kg
h	specific enthalpy, J/kg
$\dot{m}$	mass flow rate, kg/s
N	power, W
p	pressure, bar
$\dot{Q}$	heat rate, W
q	specific heat, J/kg
s	specific entropy, J/(kg K)
T	temperature, °C
v	specific volume, m^3/kg
$\dot{V}_{in}$	volume flow rate, m^3/h,
l	specific work, J/kg
x	dryness factor (steam quality), -
w	relative velocity, m/s
u	circumferential velocity, m/s

Greek symbols

α	turbine stage absolute velocity outlet angle
β	turbine stage relative velocity outlet angle
η	efficiency
ϱ	turbine stage degree of reactivity, density
μ	turbine stage flow coefficient
ϑ	turbine stage velocity ratio coefficient
ψ	rotor blade velocity coefficient
φ	nozzle velocity coefficient

Subscripts and superscripts

1, 2, 3, 4	Characteristic points of real ORC
0/1/2	Parameter at turbine stage inlet/behind nozzle/behind rotor blading
a	Ambient
br	Brine
e	Effective
g	Generator
he	Heat exchanger
i	Isentropic
in	Inlet
iso	Isobutane
m	Mechanical
net	Net power output
ORC	Organic Rankine Cycle
out	Outlet
P	Pump
s	Isentropic parameter for characteristic points
T	Turbine
t	Technical
I	First Law thermal efficiency
II	Second Law thermal efficiency

geothermal power plants in regions in which they have so far been unprofitable.

The conversion of geothermal energy into electrical energy has existed for approximately a century. In 1903, Prince Piero Ginori began research concerning the possibilities of electricity generation in Larderello, Tuscany, Italy. The first commercial geothermal power plant was built there in 1913. Most villages in the Larderello region received their electricity from direct connection with the power plant. In 1914, a 2.5 MW_e turbo-alternator, which was capable of generating electricity on an industrial scale, was connected to the power distribution system in Volterra and Pomarance. This construction was the first historical proof that electricity could be produced through the conversion of geothermal energy. It is important to remember that the first commercial binary plant of 670 kW_e was built in 1967 at Paratunka on Kamchatka Peninsula, Russia [6]. At present, the worldwide geothermal electrical capacity is now around 16 GWe. Electricity produced via geothermal energy occurs in 29 countries worldwide of which most occurs in the United State (USA – 3.7 GWe) [10]. Approximately 1.8 GWe of the power is generated in Europe, primarily in Italy (916.0 MW_e), Iceland (755.0 MW_e), Germany (43.0 MW_e), Portugal (33.0 MW_e), France (17.0 MW_e), and Croatia (16.5 MW_e) [10].

Among the geothermal technologies used for energy production, binary power plants are the most popular, with over 270 units in operation worldwide. In 2014, the total installed power of binary plants was already equal to 1726 MW_e, which represented about 14% of the geothermal power stations installed worldwide [11]. Some new propositions are also on the preliminary developing stage, such as geothermal power plants co-operating with a Hot Dry Rock system in which CO_2 is used [12].

The construction of a geothermal power station in the case of extensive resources with temperatures above 200 °C, (as is the case in Italy for example), is a proven. The situation is different in the case of sources with a lower temperature and, moreover, located deeper location. In addition, the availability of other, more competitive energy sources in the region plays an important role.

The authors of this article decided to conduct an analysis based on the example of Poland as a Central European county, with relatively small geothermal resources but focused on increasing its participation in RES. This undertaking is an extremely difficult task for a country whose energy sector is based on coal; however, the first steps to increase RES share were taken in 2009 [13]. Additional pressure with respect to this issue comes not only from European Union regulations but also from government guidelines for closing coal mines by 2049 [14].

In contrast to conventional power plants, geothermal power plants belong to the group of low-efficiency systems (5%–20%) due to a low temperature of water (brine) up to 130 °C [15]. This information has been confirmed for both the Organic Rankine (ORC) and Kalina cycles [16]. The estimates confirm that usage of the single flash geothermal power station in Polish geothermal conditions does not sufficient results to be reached, therefore, such a system is not relevant for Poland [17]. Nevertheless, binary geothermal power plants as zero-emission sources used to generate electricity can still create new alternatives for clean energy in Poland [18,19].

1.1. Potential of geothermal energy in Poland

In Poland, low-temperature geothermal resources occur, related mainly to sedimentary rocks such as sandstones, limestones, and dolomites although rarely with igneous rocks (crystalline, volcanic) [20]. Four hydro-geothermal regions characterised with different conditions can be found in Poland (Table 1). The highest geothermal potential relates to the Polish Lowlands and Podhale area as these areas are a part of the Carpathians (Table 1). Much lower perspectives relate to the area of the Carpathian Foredeep (due to low well outflows) and the remaining part of the Carpathians. In the Sudetes, geothermal waters occur in patches, and geothermal reservoirs, unlike in other regions, are formed from crystalline rocks.

Currently geothermal resources are used mostly for heating and therapeutic and recreational purposes. At the end of 2018 six geothermal district heating plants were operating, those in the Podhale

Table 1
Geothermal parameters of hydrogeothermal region in Poland [22].

	Polish Lowlands	Carpathian Foredeep	Carpathians	Sudets
Geothermal reservoir	sedimentary	sedimentary	sedimentary	crystalline
Temperature [°C]	30–130	20–120	20–120	max.86.7
Discharge of wells [m3/h]	high, locally even above 300	usually less than 20, the exception is the Cenomanian aquifer- max. ca. 250	from low in Outer Carpathians to up to 550 (Inner Carpathians – Podhale)	from several to several dozen
Mineralization [g/L]	Varied, locally high, sometimes exceeding 300	Varied, locally high, sometimes exceeding 300	from several to 120	To ca.10

region and in the municipalities of Pyrzyce, Mszczonów, Poddębice, Uniejów, and Stargard (Fig. 1). Their total installed geothermal capacity was 76.2 MW, and heat production 868 TJ. Fifteen geothermal recreation centres and ten health resorts that used geothermal water for treatment were also operating at the end of 2018. Geothermal applications also involved fish farming and some other minor uses (Fig. 1) [21].

Research of the possibilities of using geothermal resources for electricity production were conducted [18]. The most prospective region for hydro-geothermal energy utilization, including electricity production, was found to be Podhale Basin. This basin is the area in which the largest geothermal heating installation in Poland and plans for further geothermal development exist. In the Polish Lowlands the best prospects for the utilization of geothermal water in binary systems occur in the central part of Polish Lowlands in which the temperature of the water

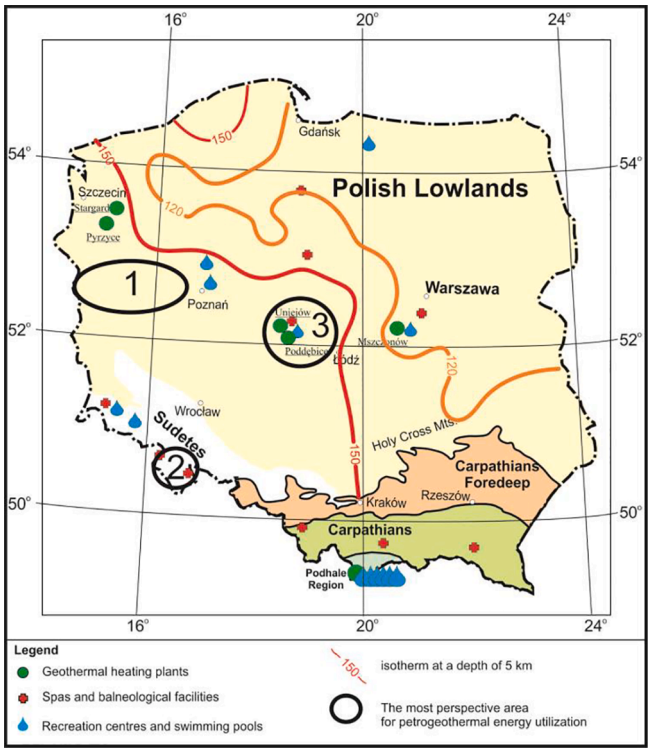

Fig. 1. The most perspective area for petro-geothermal energy utilization together with location of geothermal installations in Poland: 1 – Gorzow block area, 2 – Karkonosze pluton – Szklarska Poręba area, 3 – central part of Polish Lowlands – Krośniewice/Kutno area.

accumulated in Lower Jurassic reservoir exceeds 90 °C.

For several years, the research connected with assessment of analysis of the possibility of using petro-geothermal energy is carried out [21,23]. As the result of this research the most prospective area for geothermal power plant construction based on petro-geothermal resources have been determined [24]. Several areas have been distinguished, but three of them are the most interesting (Fig. 1): (1) Gorzow block area (volcanic rocks), (2) Karkonosze pluton – Szklarska Poręba area (crystalline rocks), (3) central part of Polish Lowlands – Krośniewice/Kutno area (sedimentary cover). In selected areas, the rock temperature at a depth of 5 km exceeds 150 °C, the thickness of the reservoir is greater than 300 m, and porosity and permeability of the reservoir rocks is very low. This parameter should positively affect the process of fracturing the reservoir and injection of the medium for the Enhanced Geothermal System (EGS).

Enhanced Geothermal Systems requires drilling to a depth where the temperature of the rocks are sufficiently hot to transfer heat into a working fluid [25]. This technology includes drilling at least two wells, creating artificial fractures in the rocks and circulating water through the man-made fractures to extract heat to the surface for electricity generation. EGS include conduction-dominated, low permeability resources [26]. This kind of resources are the subject of global research on the technology of heat recovery for power generation in binary systems, often in combination with heat production.

The mean value of the temperature increase corresponding to the depth in Poland is about 25 °C/km and changes from 16 °C/km in the northeastern part to over 30 °C/km in the northwestern Polish Lowlands [25]. As shown in Fig. 1 about 3/4 of Poland's area has a temperature above 120 °C at a depth of 5 km and about 1/2 more than 150 °C at this depth [27]. These are potential prospective areas for the construction of binary systems based on petro-geothermal energy.

Technological challenges for improving the efficiency of EGS as well as binary power plant installations still exist. However, it is certain that significant amounts of geothermal energy occur in deep petro-geothermal reservoirs [26]. Innovative technological solutions, including the reduction of deep drilling costs, will significantly improve the availability of these types of resources.

The recognition of geothermal energy as one of the Polish Government's priorities in national energy and economic development has translated into the launch of a financial backing programs for geothermal investments, by the Ministry of the Environment. The financial support for the Polish geothermal energy sector is provided mainly by the National Fund for Environmental Protection and Water Management. In the context of geothermal energy, the main goal is set as utilization of geothermal energy resources for heating purposes and generation of electricity, for the period from 2014 to 2025 [29]. At the end of September 2017, local authorities of Szaflary (Podhale region), received large subsidies from The National Fund for Environmental Protection and Water Management in order to investigate and explore geothermal resources. The production well will be drilled in with target depth of 7 km and should be ready in 2022 or at the latest in 2023 [30]. Information obtained from this drilling will bring interesting results in terms of recognition of such deep geothermal zones in Poland.

1.2. *The Organic Rankine Cycle*

Binary power plants generally operate on the basis of the classical ORC using low – boiling point working fluids. The use of alternative technology, such as the Kalina cycle, indicates the possibilities of obtaining higher efficiency (under similar working conditions) [16]. As an example of other technologies being currently under development, the conceptual project of geothermal binary power plant based on supercritical CO_2 can be mentioned [31]. Still, the majority of geothermal binary installations base on ORC [7]. Currently, various organic fluids, such as ammonia, isobutane, pentane, propane, freons and zeotropic mixtures, are being analysed [32].

In only a couple of years, several thermodynamic analyses were carried out to assess ORC performance. Many studies were performed on ORC combined not only with geothermal heat utilization, but also with solar energy utilization. Some of these studies are directly related to the present assessment. Desideri and Bidini examined three ORC configurations and investigated the effects of working fluids and their pressure at the turbine inlet in regards to ORC performance [33].

Much ORC data can be obtained from works of Ziółkowski et al. [34] and Mikielewicz et al. [35], both of whom describe hybrid cycles, mainly: steam cycle advance due to ORC introduction. However, cooperation of different kinds of cycles with ORC was also analysed in article of Kowalczyk et al. [36], which focuses on the bottoming out of the steam power plant cycle. Additionally, when forming the Szewalski cycle [37], ORC takes the heat of the condensed steam behind the main turbine. The application of such a solution usually yields a small increase in the efficiency of the entire cycle but allows for a large reduction in the size of the low-pressure part of the main turbine. All of the above-mentioned analyses refer only to thermodynamic cycles without considering geothermal sources and power station locations. However, it is worthwhile to take a closer look at the issues related to the selection of the operating medium in the ORC cycle.

Hung et al. [38] studied the ORC with different working fluids. These authors parametrically compared cryogens, such as ammonia, benzene, R11 (Trichlorofluoromethane), R12 (Dichlorodifluoromethane), R113 (Bromochlorodifluoromethane), and R134a (1,1,1,2-Tetrafluoroethane) and proved that the ORC efficiency decreases for dry fluids due to different slopes and shapes of the saturation curves [38]. Gnutek and Bryszewska proposed the ORC engine by using R123 (2,2-Dichloro-1,1,1-trifluoroethane) as a working fluid to utilize low temperature waste heat sources [39]. Wei et al. carried out numerical simulations of the ORC using R245fa (1,1,1,3,3-Pentafluoropropane) as a working fluid driven by exhaust heat [40]. Borsukiewicz and Nowak performed a thermodynamic analysis of both ORC efficiency and power for different refrigerants and geothermal sources at temperatures below 115 °C [41]. Their calculations were specifically related to Polish geothermal conditions. They reported that the effective conversion of geothermal heat to electricity is possible in Poland, if the working fluid is correctly chosen [41]. However, they did not carry out analyses to determine the size of the system and to relate it to other existing ORC systems [41]. Wang and Zhao [42] suggested that for zeotropic mixtures, a significant increase in ORC thermal efficiencies could be gained when superheating is combined with an internal heat exchanger [9]. Although many scientific reports have been published in addition to many attempts to define criteria for the optimal design of binary power plants, no comprehensive guidelines exist [43]. Planning, design, performance and impact on the environment must be individually considered for subsequent geothermal power plants [45].

Therefore, nowadays, each binary power plant is individually designed for the specific geothermal conditions in a given location, so the state of the ORC technology is quite different in comparison to conventional power plant technology [44]. Many more sophisticated methods are being used to optimise the entire cycle and the flow channels in the expander in order to achieve the highest efficiency of subsequent solutions [45].

1.3. Design of axial turbine– literature survey

A very important issue for ORC cycles is the proper selection of the turbine. In order to do so, the literature has been studied on the basis of which it should be concluded that for smaller capacities single-stage radial turbines are typically used, and for larger turbines multistage axial turbines [46]. Alternative approaches are also being developed, as in work [47], where the authors presented the design procedures for the high temperature Supercritical Organic Rankine Cycle with a two-stage radial turbine and siloxane MM (hexamethyldisiloxane) as working fluid, with applicability in the high-grade heat source.

A zero-dimensional model for the design of radial turbo-expanders for ORC applications with special reference to the estimation of losses and efficiency has been discussed by Fiaschi et al. in the paper [48]. The model applies the most recent equations of state for real fluids expanding in the ORC turbine. Moreover, this model was a starting point for 3D design of a 5 kW micro turbo expanders for small, distributed ORC power units which was analysed in [49]. On the other hand, the issue of a design criterion for axial turbines to predict their efficiency under different conditions and for different working fluids has been addressed in [50].

Increasing the efficiency of the turbine, as an essential part of the cycle, is the subject of extensive research. Khalil et. al. at their work [51] proposed a power cycle which integrates a closed Rankine cycle with an open Rankine power cycle using liquid nitrogen from a cryogenic energy storage system. As the result of the cycle proposed by Khalil et. al., the thermal efficiency was increased by 5.7%. An interesting tip carving approach was presented in [52], what is applied to mitigate the undesired aerothermal effects of the tip leakage flow. A deeper insight into the phenomena occurring in an ORC turbine was made by the authors of the article [53]. Using the example of a single-stage expander with R245fa medium and applying an optimisation algorithm, they highlight the influence of organic fluid compressibility on turbine design. They also find an increase in efficiency when using a convergent nozzle stage at temperatures below 140 °C. Moreover, the authors of paper [54] present a novel model for the determination of thermodynamic and geometrical parameters of axial ORC turbines, avoiding any reference to ideal gases or approximate Equations of State.

Due to limited literature on the subject of the design and optimization of Organic Rankine Cycle power systems considering multistage turbine design, Meroni et al. in [55] made an attempt to process design methodology and working fluid selection for these systems. The methodology proposed by Meroni et al. allows the identification of the suitable working fluid considering the trade-off between cycle and multistage turbine designs. The steady and unsteady interactions between the components of a two-stage axial turbine and effect on efficiency has been exposed at work Touil et al. [56]. Also in publication [54], the authors designed and analysed a 16 kW two-stage axial turbine operating at 92 °C using computational fluid dynamics. The obtained isentropic efficiency was 83.94%, thus increasing the efficiency of the cycle by 3.7% compared to a system with a single-stage turbine. This solution appears to be extremely beneficial, but involves a significant complication of installation.

1.4. Literature gap

The literature gap is synthesised in Table 2. It can be concluded that this work fills a gap in the form of a complete technical analysis of an ORC cycle solution with a two-stage turbine and a correctly selected geothermal energy source. However, it is worth analysing the literature gap on individual examples of publications not described in the prior subsections. Talluri and Lombardi [54] performed a design and an optimization of ORC systems with the details of the expander design but neglected information about choosing the low-temperature source. Martins et al [53] only analyzed the single-stage turbine without extending this to a two-stage flow system, and which is carried out in this paper. Al Jubori et al. [57] developed a novel efficient small-scale two-stage axial turbine for low temperature and related Organic Rankine Cycle systems. Results showed that the two-stage axial turbine configuration exhibited substantially the higher turbine performance, with overall isentropic efficiency of 83.94%, power output of 16.037 kW and ORC thermal efficiency of 14.19%, compared to 78.30%, 11.06 kW and 10.5% and the single-stage configuration respectively. Therefore, Al Jubori et al. [57] presented a general design which did not analyze heat source and geographical conditions but does affect design and turbine performance.

Da Lio et al [50] examined the single-stage turbine with the

Table 2
Summary of the literature gap in relation to the issue of designing an ORC cycle with a two-stage axial turbine and selecting a geothermal heat source.

Authors	Literature source	Analysis of heat source	Analysis of thermodynamic cycle	Analysis of turbine design
Ziółkowski et al	This research	Yes	Yes	Yes, two stages
Martins et al.	[53]	No	Yes	Yes, one stage
Al Jubori et al.	[57]	No	Yes	Yes, two stages
Da Lio et al	[50]	No	Yes	Yes, one stage
Lazzaretto and Manente	[58]	No	Yes	Yes, one stage
Kaczmarczyk et al.	[59]	No	Yes	Yes, one stage
Kaczmarczyk et al.	[60]	Yes, Boiler	Yes, steam turbine	No
Głuch and Krzyżanowski	[61]	No	Yes	Yes, multi stages
Butterweck and Głuch	[62]	No	Yes, steam turbine	Yes, diagnostic level
Klonowicz et al	[63]	No	Yes	Yes
Cavazzini and Dal Toso	[64]	Yes, boiler	Yes	No
Yamamoto et al.	[65]	No	Yes	Yes
Kotas	[66]	Yes, boiler	Yes	No
Szargut et al.	[67]	Yes, boiler	Yes	No
DiPippo	[68]	Yes, Geothermal heat source	Yes	No
Dağdaş	[69]	Yes, Geothermal heat source	Yes	No
Zare	[70]	Yes, Geothermal heat source	Yes	No
Touil and Ghenaiet	[56]	No	No	Yes
Meroni et al.	[55]	No	Yes	Yes
Maral	[52]	No	No	Yes
Khalil et al.	[51]	No	Yes	Yes
Fiaschi et al.	[49]	No	No	Yes
Fiaschi et al.	[48]	No	No	Yes
Dong et al.	[47]	No	Yes	Yes
Witanowski et al.	[46]	No	Yes	Yes
Ghasemi et al.	[45]	Yes	Yes	No
Walraven et al.	[44]	Yes	Yes	No
Moya et al.	[43]	Yes	Yes	No
Wang and Zhao	[42]	Yes	Yes	No
Borsukiewicz-Gozdur and Nowak	[41]	No	Yes	No
Wei et al.	[40]	No	Yes	No
Gnutek and Bryszewska-Mazurek	[39]	No	Yes	No
Kowalczyk et al.	[36]	No	Yes	No
Hung et al.	[38]	No	Yes	No
Mikielewicz et al.	[35]	No	Yes	No
Ziółkowski et al.	[34]	No	Yes	No
Desideri and Bidini	[33]	No	Yes	No
et al.	[32]	No	Yes	No
Gładysz et al.	[31]	No	Yes	No
Sowiżdżał et al.	[29]	Yes	No	No
Górecki et al.	[28]	Yes	No	No
Tester et al.	[26]	Yes	Yes	No
Anderson et al.	[25]	Yes	Yes	No
Sowiżdżał et al.	[23]	Yes	No	No
Kaczmarczyk et al.	[16]	Yes	Yes	No
Madhawa et al.	[15]	Yes	Yes	No
Loloum et al.	[13]	Yes	No	No
Tomasini-Montenegro et al.	[12]	Yes	Yes	No
DiPippo	[11]	Yes	Yes	No
Huttrer	[10]	Yes	Yes	No
Cataldi	[9]	Yes	Yes	No
Wachowicz-Pyzik et al.	[7]	Yes	Yes	No
DiPippo R	[5]	Yes	Yes	No
Barbacki and Pająk	[17]	Yes	Yes	No
Sowiżdżał	[20]	Yes	No	No
Kępińska	[21]	Yes	Yes	No
Sowiżdżał et al.	[22]	Yes	No	No

presentation of performance maps whereas did not take into consideration a flow turbine with more stages. Lazzaretto and Manente [58] carried out detailed thermodynamic and basic design calculations but did not plot velocity triangles. Kaczmarczyk et al [59,60] presented an experimental study of a low-temperature micro-scale ORC. This turbine is in much smaller scale than issues analysed in this paper, regarding completely different heat source, namely boiler. This solution allows a cogeneration of heat and electricity for domestic application; however, it is not appropriate for geothermal systems. The breakdown risk assessment is especially important in ORC turbines because many of

them work in aggressive conditions and long-term interaction between various refrigerants and blades which are not as well recognized for water. Głuch and Krzyżanowski [61] concept and procedures of the diagnostic system based on thermal measurements for classical steam turbines are not extended to the design of ORC turbines. The application of neural networks in turbine diagnostic is an interesting and promising topic. Butterweck and Głuch [62] presented an application method of artificial neural networks to perform the fluid flow calculations through both damaged and undamaged turbine blading. Nevertheless, a proper approach to geothermal heat source and ORC turbine design needs to be caried out.

Klonowicz et al. [63] has proposed the selection procedure of optimum degree of partial admission depending on the tip clearance. A case study has been presented for a micro-turbine designed for an operation in a micro CHP unit running with HFE 7100 working fluid, nevertheless this is a general design method. Authors do not analyse a heat source.

Cavazzini and Dal Toso [64] performed a techno-economic feasibility analysis of the integration of a small-scale commercial ORC in a real case study, represented by a highly-efficient industrial distillery. However, authors did not take into account the turbine design. Yamamoto et al. [65] demonstrated ORC for the low temperature source, but did not consider the geothermal heat source and turbine design. Kotas [66] established a general exergy analysis for a simple process. Szargut J. et al. [67] also yielded principles of exergy analysis. DiPippo [68] presented a comparision between operating Kalina and ORC power plants. In addition, he did not analyse possible locations for geothermal power plants neither turbine design.

Dağdaş et al. [69] showed analysis of the Denizli single flash geothermal power and compared it to the binary power plant. This geothermal power plant has a relatively high heat source temperature contrary to this article. Furthermore, the authors did not examine the design of the turbine.

A comparative exergoeconomic analysis of three different ORC configurations was investigated by Zare [70]. He did not study the turbine design nor possible location of new low temperature ORC binary power plants. Kowalczyk et al. [71] analysed a cooperation of steam cycle with ORC using First and Second Law of Thermodynamics. Whereas they did not take into account design aspets of turbine blade and kinetics of flow with velocity triangles.

Ziółkowski et al. [72] developed a numerical model for utilization of waste heat from the power plant by use of the ORC. First Law of Thermodynamics was included in this approach, however ORC turbine was not designed.

Touil and Ghenaiet [56] proposed different methodologies for the expander design; however, the influence of cycle was set to a constant value in all cases. This work [56] only analyzes the axial turbine design. Moreover, Meroni et al. [55] considered ORC thermodynamical cycle and turbine design but neglected a heat source analysis. Maral et al. [52] presented a method for optimization of tip carving for an axial turbine blade with genetic alghoritm, but did not cover thermodynamical cycle nor heat source. Khalil et al. [51] only investigated non-repeated annular area dual stage small-scale nitrogen axial turbine for hybrid open-closed Rankine cycle. Fiaschi et al. [49] evaluated design of micro radial turboexpanders for ORC power cycles. They did not study heat source nor thermodynamical cycle. Fiaschi et al. in next article [48] also did not analyse heat source and thermodynamic cycle, however, they created turboexpander characteristics in a wide range. Dong et al. [47] presented performances of the supercritical Organic Rankine Cycle and the radial turbine design for high temperature applications. They did not analyzed heat source. Witanowski et al. [46] introdiused optimization method of an axial turbine for a ORC waste heat recovery system. They did not investigated heat source and thermodynamic cycle. In contrary to this research small scale system was analysed.

Wang and Zhao [42] conducted the comprehensive analyses of the upper heat source transferring heat to the cycle; however, none of the above works included the design of an axial turbine. Borsukiewicz-Gozdur and Nowak [41] introduced a different cycle configuration in ORC systems and methodologies for selecting the optimal working fluid, whereas the isentropic turbine efficiency was always set to a fixed value and analysis of low-temperature source was neglected.

Wei et al. [40] inspected only thermodynamic cycle analysis. Study for heat source is not presented. Kowalczyk et al. [36] studied bottoming SRC and ORC for modular the High Temperature Reactor. This application is different from the geothermal power plant. Authors did not design turbine geometry. Hung et al. [38] evaluated six other fluids which could be used in low grade waste heat. Unfortunately, analysed refrigerants are now withdrawn due to a high environmental impact. Mikielewicz et al. [35] developed a method for the utilisation of waste heat from the power plant with carbon capture unit by a use of the ORC. ORC turbine was not designed in that study. Blaise et al. [32] evaluated the influence of the working fluid properties on the optimized power of phase changing Carnot engine. This is the general study which does not cover specific design of ORC turbine nor geothermal energy. Gładysz et al. [31] performed a techno-economic assessment of a combined heat and power plant integrated with carbon dioxide removal. Authors designed enhanced geothermal system that can capture carbon dioxide. Turbine geometry was not constructed.

Sowiżdżał et al. [22] performed the detailed low-temperature heat source analyses for geo-thermal applications while mentioned authors did not take into consideration the thermodynamic cycle and design of axial stage turbine. The situation is similar in the work of Kępińska [21]. Sowiżdżał et al. [29] focuses on raising funds to develop the use of geothermal energy, but lacks the details of a technical solution to produce electricity. Loloum et al [13] refers to political aspects without prior detailed technical analysis. A general state of knowledge about geothermal sources in Poland was presented in [20], although no technical solution was mentioned. The work of Górecki et al. [28] was prepared in a similar approach.

The presented study in this article fills the gaps of previous articles (Table 2). It shows that it is possible to build a specific type of binary ORC power plant in the area of the Central Europe. This is important because the geothermal energy is independent on weather conditions and does not need to be backed up by the energy storage or gas turbines. Moreover, developed issues are very significant from the point of view of the electricity grid.

The article is a complete work providing valuable technical contributions for reconsidering the development of a geothermal-based electricity system in Central Europe and worldwide locations with low-temperature geothermal energy sources. Due to this fact, it introduces a comprehensive analysis in the design of a geothermal power station. Additionally, currently substantial electricity generation from geothermal energy is not considered as a part of strategy for decarbonisation of Polish power system.

1.5. Aims, research hypothesis and scope of the article

Based on the available knowledge of the authors and the undertaken literature studies the main novelty of the present work is the combination of three issues, namely the selection of the low- temperature heat source, the design and analysis of the cycle together with a turbine adapted to these conditions.

Even with the low-temperature heat sources used so far mainly for heating, balneotherapy and recreation purposes it is possible to design a binary power plant that would be valid from a thermodynamic point of view. This hypothesis addresses the need to develop environmentally friendly power plants using renewable energy sources with geothermal energy. The design and construction of geothermal power plants becomes particularly relevant in the context of world politics, including the European Union, where consortia are being formed around clean energy technologies. Additionally, currently substantial electricity generation from geothermal energy is not considered as a part of strategy for decarbonisation of Polish power system. The general problem

which is solved in this article concerns the combined design of an ORC cycle and turbine based on low temperature heat source specifications.

This article shows the application of a binary geothermal power plant under Polish conditions. Despite the lack of popularity of this solution it is possible to build such power plant not requiring an extraordinary level of technology. The goal was achieved by not only identifying optimal regions, but also by thermodynamic analysis of the power plant cycle and a preparation of a preliminary turbine design.

Based on the preceding literature analysis, it was decided to define a heat source corresponding to the resources of the Polish Lowlands and Carpathians regions after estimating a temperature of 120 °C and a mass flow of 400 m^3/h.

In order to establish a baseline, the authors performed calculations for ORC without regeneration and superheating. Following this approach, the calculations for the turbine stages were also made using the classical method [73,74], despite the extensive literature on new solutions. This method leaves room for further considerations, more detailed work in the field of variant and methodological analyses.

For such assumptions, both the First and Second Law of Thermodynamics thermal efficiencies were estimated. All calculations were performed by means of an in-house code. The methodology for the design calculations is presented in Section 2: Models of Organic Rankine Cycle and the axial turbine. Selected results and associated assumptions along with the resulting geometry are presented in Section 3. A discussion of the results can be found in Section 4: Scenario for establishing a binary power plant in Poland. It is worth highlighting some of the issues here, namely: 1) the estimated efficiencies were compared to efficiencies of other binary plant worldwide, which are currently working or were already dismantled; 2) based on these values, results of the designed axial turbine were contrasted with other solutions; 3) the obtained parameters of the power plant are compared with other existing geothermal power plants. All the considerations contained in the article are summarized in Section 5.

2. Models of Organic Rankine Cycle and the axial turbine

Due to low temperature, the geothermal fluid in binary power plants cannot be directly used to produce electricity, as for instance it is in other power stations (dry steam or single and double flash systems). However, the thermal energy available in the geothermal fluid can be used (see Fig. 2 – primary and secondary cycle) to vaporize a working fluid in thermal cycle (isobutane, n-isobutane, n-isopentane and pentane). Typically, a thermodynamic Organic Rankine Cycle or Kalina cycle is used to produce electricity [6,47]. In most cases, such power stations operate with two – well systems in primary cycle. Figs. 2 and 3 present the technical realization and the schematic *T - s* diagram for the simplified ORC.

As it is well known, the ORC consists of four thermal processes:

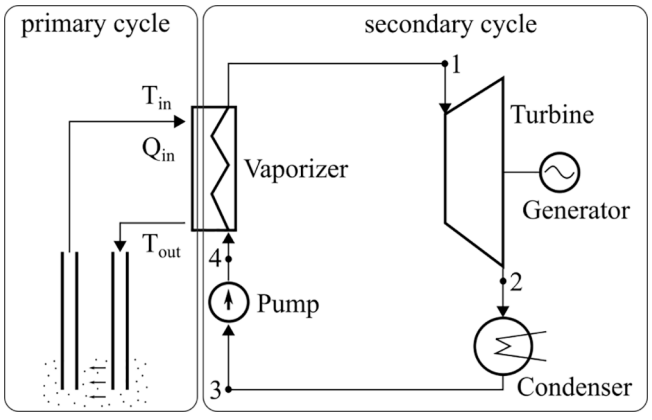

Fig. 2. Scheme of the ORC technical realization.

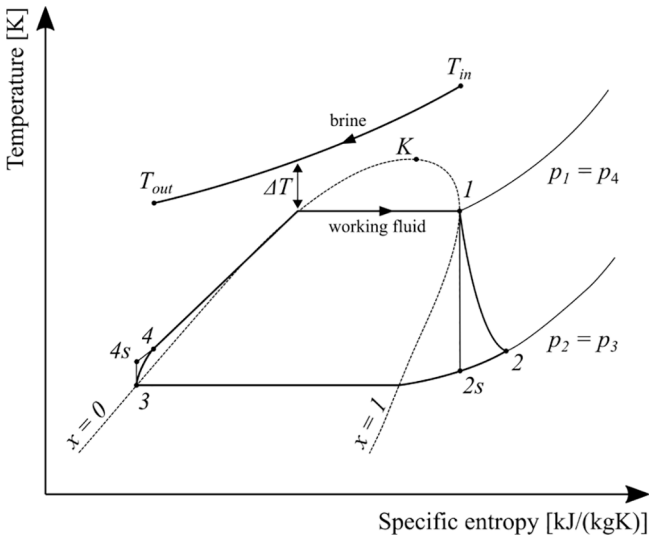

Fig. 3. Schematic diagram of simple ORC; x – steam quality, K – critical point.

1-2 - isentropic expansion in the turbine,
2-3 - heat rejection at constant pressure in the condenser,
3-4 - isentropic compression by the pump,
4-1 - heat supply at constant pressure in the vaporizer.

As presented above and as shown in Figs. 2 and 3, the geothermal fluid (brine) heats the working fluid in the vaporizer (*V*), which later expands in the turbine (*T*) and condenses in the condenser (*C*) at the condenser pressure. Finally, the pump (*P*) causes an increase in the pressure of the working fluid.

In the analysis, isobutane was chosen as the working fluid because it is a natural refrigerant, has good thermodynamic properties, and its global warming potential (GWP) and ozone depleting potential (ODP) are very low [34]. Its ODP is 0 and the GWP is equal to 3. For example fluids R245fa and R236fa (1-Chloro-1,1,3,3,3-pentafluoropropane) also have good thermodynamic properties, but their GWPs are 1030 and 9810 respectively. Basic physical and thermodynamic data of isobutane R600a (isobutane) were obtained from National Institute of Standards and Technology (NIST) [75] and are given in Table 3.

2.1. Organic Rankine Cycle calculations

The first step in the cycle calculations is to determine a heat flux delivered to the cycle by the brine in the steam generator required to vaporize isobutane:

$$\dot{Q}_r = c_{p,br}\rho\dot{V}(T_{in} - (T_1 + \Delta T)) \quad (1)$$

Next, taking h_1' as the enthalpy of onset of evaporation (for $x = 0$) and using a latent heat of isobutene

$$q_r = h_1 - h_1' \quad (2)$$

Table 3
Physical and thermodynamic data for isobutane based on the National Institute of Standards and Technology [71].

Parameter	Value	Unit
Molecular weight	58.123	kg/kmol
Critical pressure	36.29	bar
Critical temperature	134.66	°C
Critical density	225.55	kg/m^3
Normal boiling point	−11.749	°C
Autoignition temperature	460	°C
Thermal conductivity (1.013 bar and 0 °C)	0.0139	W/(mK)
Ratio of specific heats (1.013 bar and 0 °C)	1.0958	–

there can be specified a mass flux of isobutane in the cycle:

$$\dot{m}_{iso} = \frac{\dot{Q}_r}{q_r}. \tag{3}$$

Heat flux required to heat the isobutane from temperature T_4 to T_1' is described as:

$$\dot{Q}_h = \dot{m}_{iso}(h_1' - h_6), \tag{4}$$

giving liquid temperature at steam generator outlet:

$$T_{out} = (T_1 + \Delta T) - \frac{\dot{Q}_h}{c_{p,br}\ \rho\ \dot{V}}. \tag{5}$$

The specific work obtained during this cycle is equal to the specific work performed by the turbine l_T and reduced by the specific work absorbed by the pumpl_P, as shown below:

$$l_{ORC} = l_T - l_P = l_{t1-2s} - l_{t4s-3} \tag{6}$$

The thermal efficiency of the simplified ORC is defined as the ratio of the specific work l_{ORC} to the specific heat q_{in} in the vaporizer, as follows:

$$\eta_{ORC} = \frac{l_{ORC}}{q_{in}} \tag{7}$$

For the ideal thermodynamic processes, the specific work and specific heat are defined as a difference between inlet and outlet enthalpy, as follows:

$$\eta_{ORC} = \frac{(h_1 - h_{2s}) - (h_{4s} - h_3)}{h_1 - h_{4s}} \tag{8}$$

In practice, both the higher pressure and temperature of the working fluid at the turbine inlet and lower pressure at the condenser lead to a higher cycle efficiency.

The endpoint of either expansion or compression in real processes is significantly different from the ones that occur in ideal machines, so the degree of irreversibility of both the isentropic compression and the expansion is usually defined by an internal efficiency,η_{iP} and η_{iT}, as follows [66,67]:

$$\eta_{iP} = \frac{l_{t3-4s}}{l_{t3-4}} \tag{9}$$

$$\eta_{iT} = \frac{l_{t1-2}}{l_{t1-2s}} \tag{10}$$

This process leads to the conclusion that the overall power plant efficiency η_I is always lower than the thermal efficiency of the cycle :

$$\eta_I \leq \eta_{ORC} \tag{11}$$

The overall power plant efficiency η_I is defined, as follows [5]:

$$\eta_I = \frac{N_{net}}{\dot{Q}_{in}} \tag{12}$$

It should be noted that the overall power plant efficiency η_I is evaluated based on the First Law of Thermodynamics and therefore can be called a First Law thermal efficiency.

The net power output of the binary power plant N_{net} is defined, as shown below [5]:

$$N_{net} = \eta_m \eta_g N_e \tag{13}$$

in which: η_m is mechanical efficiency, η_g represents generator efficiency, and N_e is the effective power. N_e is calculated using the formula [5]:

$$N_e = \dot{m}_{iso}\left(l_T \eta_{iT} - \frac{l_P}{\eta_{iP}}\right) \tag{14}$$

where: $\dot{m}_{iso}$ is mass flow rate of isobutane.

It is also very useful to define the overall plant efficiency by means of an exergy definition and the Second Law of Thermodynamics. The Second Law thermal efficiency can determined shown in Eq. (15) [68]:

$$\eta_{II} = \frac{N_{net}}{\dot{m}_{br} e_{br,in}} \tag{15}$$

where: $\dot{m}_{br}$ is mass flow rate of brine and $e_{br,in}$ is brine specific exergy at vaporizer inlet.

The specific exergy of brine $e_{br,in}$ is defined in Eq. (16) [66]:

$$e_{br,in} = c_{p,br}\left[(T_{in} - T_{out}) - T_a \ln\left(\frac{T_{in}}{T_{out}}\right)\right] \tag{16}$$

where: brine inlet temperatureT_{in} = 393 K, and ambient temperature T_a = 293 K. For brine, zero exergy is taken to correspond to the brine outlet temperatureT_{out} = 293 K.

2.2. Axial turbine stage theory

Turbine stage calculations were performed according to the model presented in [73,74]. In this case, the subscripts 0, 1 and 2 indicate the value at the inlet to the turbine stage, the value behind the nozzle blades and the value behind the rotor blades, respectively. Fig. 4 presents the axial turbine flow diagram with parameters describing the velocities and directions of the medium. On their basis, medium velocity vectors were calculated and then drawn and are presented as velocity triangles as shown in a compact form in Fig. 5.

2.3. Mathematical model for design of axial turbine

A proposed calculation procedure should be as simple as possible and can be repeated many times with the need for an optimisation process. Calcuations of the two turbine stages are presented below:

- enthalpy of isentropic drop behind a nozzle, assuming h_s and ρ,

$$h_{1s} = h_0 - h_s \cdot (1 - \rho), \tag{17}$$

- enthalpy isentropic drop in a rotor row,

$$h_{sr} = \rho \cdot h_{s,} \tag{18}$$

- enthalpy isentropic drop in a nozzle,

$$h_{sn} = (1 - \rho) \cdot h_s, \tag{19}$$

- relative circumferential speed with the assumed velocity ratio coefficient ϑ,

$$u = \vartheta \cdot \sqrt{2 \cdot h_s}, \tag{20}$$

- average diameter of the blade row,

$$d_{av} = \frac{60 \cdot u}{\pi \cdot n}, \tag{21}$$

- entropy of isentropic drop behind a nozzle – equal to entropy before the turbine,

$$s_{1s} = s_0, \tag{22}$$

- pressure behind a nozzle as obtained from the steam tables,

$$p_1 = p(h_{1s}, s_{1s}), \tag{23}$$

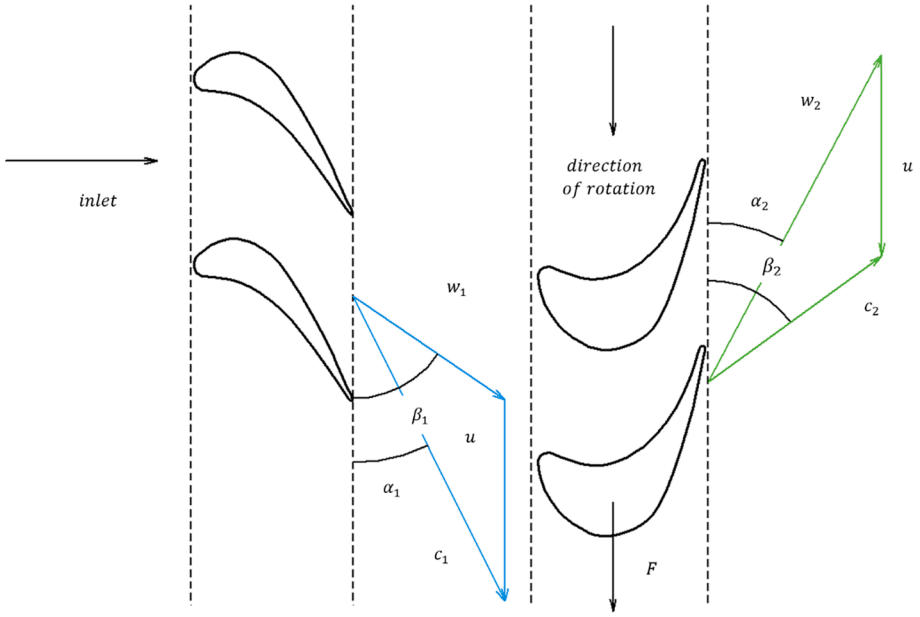

Fig. 4. The axial turbine flow diagram.

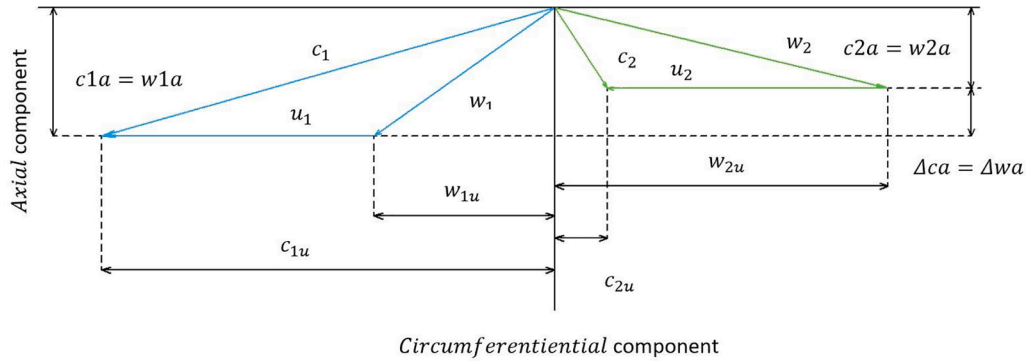

Fig. 5. Velocity vectors of the axial turbine stage.

- absolute velocity of medium before a nozzle, which is assumed to be zero ($c_0 \approx 0$),

$$c_0 = 0\ \frac{m}{s}, \tag{24}$$

- absolute speed behind a nozzle with an enthalpy isentropic drop,

$$c_{1s} = \sqrt{2{\cdot}1000{\cdot}h_{sn} + {c_0}^2}, \tag{25}$$

- absolute speed behind a nozzle, with the assumed absolute nozzle velocity coefficient φ,

$$c_1 = c_{1s}{\cdot}\varphi, \tag{26}$$

- enthalpy of the medium behind a nozzle,

$$h_1 = h_0 + \frac{{c_0}^2}{2} - \frac{{c_1}^2}{2}, \tag{27}$$

- entropy behind a nozzle, equal to entropy of an isentropic drop behind the rotor palisade – read the from steam tables,

$$s_1 = s_{2s} = s(p_1, h_1), \tag{28}$$

- enthalpy behind a rotor row with an enthalpy isentropic drop,

$$h_{2s} = h_1 - h_{sr}, \tag{29}$$

- pressure behind the rotor row – read from the steam tables,

$$p_2 = p(h_{2s}, s_1), \tag{30}$$

- relative velocity of the medium behind a nozzle, with the α_1 angle assumed,

$$w_1 = \sqrt{{c_1}^2 + u^2 - 2{\cdot}c_1{\cdot}u{\cdot}cos\alpha_1}, \tag{31}$$

- relative speed vector angle behind a nozzle,

$$\beta_1 = arcsin\left(\frac{c_1{\cdot}sin\alpha_1}{w_1}\right), \tag{32}$$

- relative velocity behind the rotor row with enthalpy isentropic drop,

$$w_{2s} = \sqrt{2{\cdot}1000{\cdot}h_{sr} + {w_1}^2}, \tag{33}$$

- relative velocity behind the rotor row, with the assumed blade velocity coefficient,

$$w_2 = w_{2s} \cdot \psi, \tag{34}$$

- enthalpy drop in a nozzle,

$$\Delta h_n = h_1 - h_{1s}, \tag{35}$$

- enthalpy loss in a nozzle,

$$\Delta h_r = \left(1 - \psi^2\right) \cdot \left(h_{sr} + \left(\frac{w_1^2}{2 \cdot 1000}\right)\right), \tag{36}$$

- enthalpy of the medium behind the rotor row,

$$h_2 = \Delta h_r + h_{2s}, \tag{37}$$

- entropy behind a rotor row,

$$s_2 = s(p_2, h_2), \tag{38}$$

- specific volume of the medium behind the rotor row at enthalpy isentropic drop – read from the steam tables,

$$v_{2s} = v(p_2, s_{2s}), \tag{39}$$

- specific volume behind a nozzle at enthalpy isentropic drop,

$$v_{1s} = v(p_1, s_0), \tag{40}$$

- length of a nozzle blade,

$$l_n = \frac{\dot{m} \cdot v_{1s}}{\mu_1 \cdot \pi \cdot d_{av} \cdot c_{1s} \cdot sin\alpha_1}, \tag{41}$$

- length of a rotor blade,

$$l_r = l_n + 2 \text{ mm}, \tag{42}$$

- relative speed vector angle behind the rotor row with the assumed flow coefficient in the rotor row μ_2,

$$\beta_2 = arcsin\left(\frac{\dot{m} \cdot v_{2s}}{\mu_2 \cdot d_{av} \cdot \pi \cdot w_{2s} \cdot l_r}\right), \tag{43}$$

- absolute speed behind the rotor row,

$$c_2 = \sqrt{(w_2 \cdot sin\beta_2)^2 + (w_2 \cdot cos\beta_2 - u_2)^2}, \tag{44}$$

- angle of absolute speed vector behind the rotor row,

$$\alpha_2 = arcsin\left(\frac{w_2 \cdot sin\beta_2}{c_2}\right), \tag{45}$$

- enthalpy exhaust loss,

$$\Delta h_{ex} = \frac{c_2^2}{2 \cdot 1000} = \frac{\left(\frac{m}{s}\right)^2}{2 \cdot 1000}, \tag{46}$$

- degree of stage reaction at the hub of the rotor row,

$$\rho_h = 1 - (1 - \rho) \cdot \left(\frac{d_{av}}{d_{av} - l_r}\right)^{1,8}, \tag{47}$$

- velocity of sound propagation for the ideal flow in the medium behind a nozzle – read from the function of pressure and enthalpy,

$$a_{1s} = a(p_1, v_{1s}), \tag{48}$$

- Mach number for the ideal flow behind a nozzle,

$$Ma_{c1s} = \frac{c_{1s}}{a_{1s}}, \tag{49}$$

- velocity of sound propagation for the ideal flow in the medium behind the rotor row – read from the function of pressure and enthalpy,

$$a_{2s} = a(p_2, v_{2s}), \tag{50}$$

- Mach number for the ideal flow behind the rotor row,

$$Ma_{r2s} = \frac{w_{2s}}{a_{2s}}, \tag{51}$$

- theoretical specific work of the first (or intermediate) stage and the last stage,

$$l_{u_t} = h_s + \frac{{c_0}^2 - {c_2}^2}{2 \cdot 1000}, l_{u_t} = h_s + \frac{{c_0}^2}{2 \cdot 1000}, \tag{52}$$

- specific work of the stage,

$$l_u = h_s + \left(\frac{{c_0}^2}{2 \cdot 1000}\right) - (\Delta h_n + \Delta h_r + \Delta h_{ex}), \tag{53}$$

- stage efficiency,

$$\eta_u = \frac{l_u}{l_{u_t}}. \tag{54}$$

To determine the internal efficiency of the turbine η_{iT}, first the individual losses were calculated:

- leakage loss coefficient in the nozzle blade seals with assumed average seals diameter, d_{se}, equal to 0.3 and 0.4 m for first and second stages, respectively;

$$\xi_n = \frac{3 \cdot 10^{-4}\left(1 + \frac{0,25}{d_{se}}\right) d_{se}^2 \sqrt{1 + 1,8\frac{l_r}{d_{av}}}\eta_u}{d_{av} l_w sin\alpha_1}, \tag{55}$$

- leakage loss above rotor blades:

$$\xi_r = \frac{5 \cdot 10^{-4}\left(1 + \frac{0,25}{d_{av} + l_r}\right)\left(2 + \frac{d_{av}}{l_r} + \frac{l_r}{d_{av}}\right)\sqrt{\frac{\varrho}{1-\varrho} + 1,8\frac{l_r}{d_{av}}}\eta_u}{sin\alpha_1}, \tag{56}$$

- friction losses of rotor discs:

$$\xi_f = \frac{6 \cdot 10^{-4}\left(1 - \frac{l_r}{d_{av}}\right)^5 \vartheta^3}{\sqrt{1 - \varrho}\ \frac{l_r}{d_{av}} sin\alpha_1}. \tag{57}$$

3. Results

The thermal efficiency and the specific work of the ORC usually depend on both the temperature and pressure of the fluid at the turbine inlet as well as the pressure at the condenser. This section provides an analysis of the influence of pressure on the ORC performance. In order to

omit complicated heat exchanger calculations, commonly used parameters were adopted [35], which should ease the design process in the future. Thus, minimum pitch point temperature difference at vaporizer $\Delta T = 3\ ^{\circ}C$ was taken and the difference between the upper temperatures of the fluids was estimated to be equal $20^{\circ}C + \Delta T$. In sum, several assumptions were made:

- brine temperature and pressure at vaporizer inlet, $T_{in} = 120\ ^{\circ}C$, $p_{in} = 3$ bar,
- brine heat capacity and brine volume flow rate, $c_{p,br} = 4.22\ kJ/(kgK)$, $\dot{V}_{in} = 400\ m3/h$,
- minimum pitch point temperature difference at vaporizer, $\Delta T = 3\ ^{\circ}C$ (brine – isobutane).
- isobutane temperature at turbine inlet, $T_1 = 97\ ^{\circ}C$,
- saturation temperature in condenser and ambient temperature, $T_3 = 22\ ^{\circ}C$, $T_a = 20\ ^{\circ}C$,
- brine salinity is neglected.

For the above parameters, the calculated isobutane flux was $\dot{m}_{iso} = 41.58$ kg/s, with brine outlet temperature T_{out} of 82 °C.

3.1. Organic Rankine Cycle analysis

Generally, the discussion involving the influence of the pressure p_1 at the turbine inlet on thermal efficiency of the ORC is conducted under the assumption that both temperature T_1 at the turbine inlet and pressure p_3 in the condenser remain constant [65].

Hence, the results of the ORC are presented at different pressure and both fixed temperatures at the turbine inlet and the condenser pressure. In all cases the turbine inlet and the condenser temperatures were equal to $T_1 = 97\ ^{\circ}C$ and $T_3 = 22\ ^{\circ}C$ respectively, while the turbine inlet pressure changes in the range of $p_1 = 9$ to -18.716 bar. It should be noted that the pressure $p_1 = 18.716$ bar corresponded to the saturation temperature was equal to $T_1 = 97\ ^{\circ}C$. Whenever the turbine inlet parameters have achieved saturation conditions, the calculations for a different isobutane dryness factor x_1, in the range of 0.8–1.0 were performed.

Results of the thermodynamic analysis are presented in Fig. 6. As it is shown, an increase of turbine inlet pressure at a fixed inlet temperature leads to an increase of both the thermal efficiency and specific work. The highest values for both specific work and thermal efficiency have been obtained for saturation parameters, i.e.: T_1=97 °C, p_1=18.716 bar and $x_1 = 1$. A further decline in the dryness factor up to $x_1 = 0.8$ will lead to a decrease in both thermal efficiency and specific work. The ORC parameters characterized by both maximal thermal efficiency and specific work are included in Table 4.

3.2. Axial turbine parameters

The input and output parameters of the isobutane turbine were the parameters of the medium at points 1 and 2 of the ORC. Calculations have been made for rotational speed conducive to cooperation with generators in the power system $n = 3000$ rev/min. Assumed construction parameters, presented in Table 5 and the number of stages had been obtained iteratively so that both the length of the nozzle and rotor blades, as well as the Mach number were designedly acceptable values.

In addition, the inlet enthalpy $h_0 = 674.33$ kJ/kg of the first stage equals the enthalpy before the turbine, and for the next stage equals the outlet enthalpy h_2 of the previous stage. The same is the case with the absolute inlet speed c_0, estimated for the first stage at 36.71 m/s, and for the next stage equal to the absolute outlet speed c_2 of the previous stage.

Table 6 and 7 show results of detailed thermodynamics calculations of turbine stages. The chosen low reactivity of the stages indicates an impulse type turbine with a disc structure. Many ORC turbines has centrifugal structure, however their power and mass flux of working liquid is multiple times lower than in analysed case. For high power and mass flux applications axial turbines achieve higher efficiency than

Table 4
Thermodynamic parameters of ORC for maximal thermal efficiency and specific work – reference cycle interpreted in Fig. 3.

Point	Temperature, °C	Pressure, bar
1	97	18.716
2	34	3.225
3	22	3.225
4	24	18.716

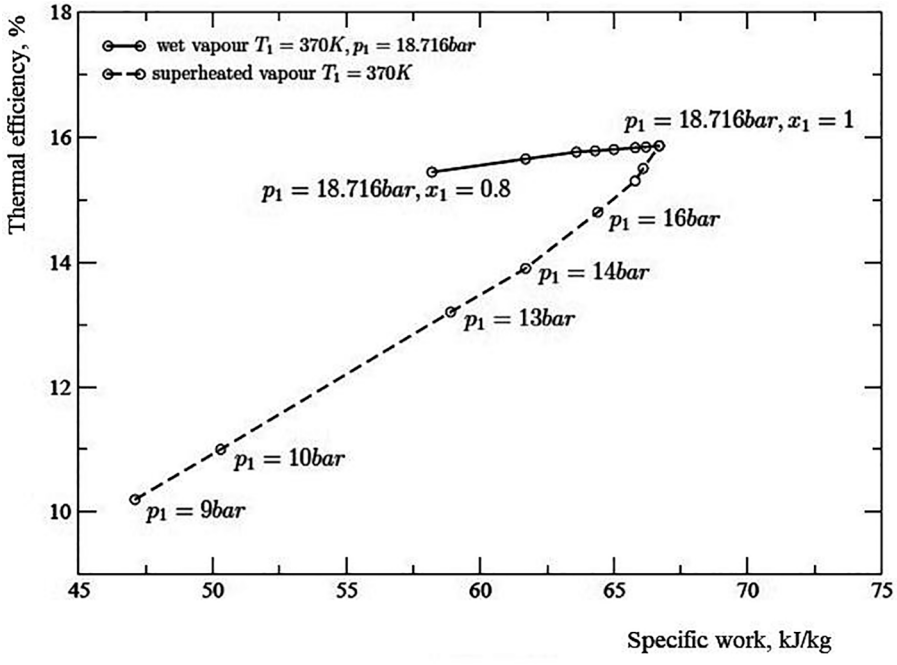

Fig. 6. The thermal efficiency η_{ORC} vs. specific workl_{ORC}.

Table 5
Assumptions for turbine stage calculations.

Parameter	Symbol	Unit	Value	
Stage number	–	–	1	2
Isentropic enthalpy drop	h_s	kJ	28.130	41.309
Degree of reactivity	ϱ	–	0.100	0.100
Nozzle flow coefficient	μ_1	–	0.930	0.930
Rotor flow coefficient	μ_2	–	0.930	0.930
Velocity ratio coefficient	ϑ	–	0.464	0.470
Nozzle outlet angle	α_1	°	10	13
Rotor blade velocity coefficient	ψ	–	0.950	0.950
Nozzle velocity coefficient	φ	–	0.950	0.950

radial ones. Authors have chosen impulse turbine over reaction turbine because it has simpler construction. Tip leakage loses and axial force on rotor are lower on impulse turbines. This allows to adapt simpler sealings and simpler system for axial force compensation, what contributes to lower investment costs [69]. Design and construction of drum for reaction turbines is much more demanding than discs for impulse ones, what increase investment cost. Furthermore stages of impulse turbines could be more loaded than reactive stages. Because of all above advantages authors decided to choose axial impulse turbine for construction.

Turbine consists of form two stages. Reaction ratio of each stage is 10%, because lower value could result in ventilator work for work under partial load. Expansion begins at 0.961 MPa and ends at 0.323 MPa. Isentropic enthalpy drop at stage 1 is 28.13 kJ/kg and isentropic enthalpy drop at stage 2 is 41.31 kJ/kg. Efficiency of stage one is 86.4% and efficiency of stage 2 is 81.8%. Efficiency of second stage is lower because outlet velocity of second stage cannot be reworked in next stage.

Mean diameter for the first stage is 0.755 m and mean velocity for the second stage is 0.867 m. Length of rotating blades is low and varies from 0.023 m for the first stage to 0.035 m for rotor of the second stage. Outlet velocity c_2 is rather low to reduce outlet loss. High Mach numbers, appearing behind the nozzles of both stages, define the flow in this place as supersonic – this is an undesirable phenomenon, but often occurring in the design of low-boiling medium turbines [46,63]. The determined absolute velocities c_1, c_2, circumferential velocities u_1, u_2 and the relative velocities of the medium w_1, w_2, as well as α and β angles, allowed the characterization of both turbine stages using velocity triangles (according to Fig. 6), which is shown in Fig. 7. Experience form construction of industrial steam turbines could be used in analysed case because similar values of kinematic parameters are frequently encountered their designs.

Shape of velocity triangles is typical for impulse turbine stages. Values of degrees α and β do not exceed typical conditions which occur inside steam turbines, what indicate that conventional blade profiles could be applied in analysed case.

3.3. Losses and efficiency of axial turbine

The values of individual losses are presented in Table 8. Then, by determining the internal efficiency η_i and internal specific work l_i of both stages, the internal efficiency of the turbine was calculated at $\eta_{iT} =$ 81%, which coincides with the value assumed for ORC.

$$\eta_i = \eta_u - \xi_n - \xi_r - \xi_f, \tag{58}$$

$$l_i = \eta_i (h_0 - h_{2s}), \tag{59}$$

Table 6
Turbine stage thermodynamics calculation results.

Equation No.	–	(12)	(13)	(14)	(17)	(18)	(22)
Parameter	$h_0 \left[\frac{kJ}{kg}\right]$	$h_{1s} \left[\frac{kJ}{kg}\right]$	$h_{sr} \left[\frac{kJ}{kg}\right]$	$h_{sn} \left[\frac{kJ}{kg}\right]$	$s_{1s} \left[\frac{kJ}{kg \cdot K}\right]$	p_1 [MPa]	$h_1 \left[\frac{kJ}{kg}\right]$
#1 stage	674.33	649.015	2.813	25.317	2.3755	0.9614	651.55
#2 stage	649.51	612.331	4.131	37.179	2.3852	0.3600	616.01

Equation No.	(23)	(24)	(25)	(30)	(31)	(32)	(33)
Parameter	$s_1 \left[\frac{kJ}{kg \cdot K}\right]$	$h_{2s} \left[\frac{kJ}{kg}\right]$	p_2 [MPa]	$\Delta h_n \left[\frac{kJ}{kg}\right]$	$\Delta h_r \left[\frac{kJ}{kg}\right]$	$h_2 \left[\frac{kJ}{kg}\right]$	$s_2 \left[\frac{kJ}{kg \cdot K}\right]$
#1 stage	2.3829	648.737	0.8962	2.5341	0.7732	649.51	2.3852
#2 stage	2.3969	611.881	0.3255	3.6815	1.4338	613.31	2.4015

Equation No.	(41)	(42)	(47)	(48)	(49)
Parameter	$\Delta h_{ex} \left[\frac{kJ}{kg}\right]$	ρ_h [–]	$l_{u_s} \left[\frac{kJ}{kg}\right]$	$l_u \left[\frac{kJ}{kg}\right]$	η_u [–]
#1 stage	0.5801	0.0485	28.223	24.916	0.8828
#2 stage	2.1298	0.0207	41.890	34.644	0.8270

Table 7
Turbine stage kinematic calculation results.

Equation No.	(15)	(16)	(19)	(20)	(21)	(26)	(27)
Parameter	$u \left[\frac{m}{s}\right]$	d_{av} [m]	$c_0 \left[\frac{m}{s}\right]$	$c_{1s} \left[\frac{m}{s}\right]$	$c_1 \left[\frac{m}{s}\right]$	$w_1 \left[\frac{m}{s}\right]$	β_1 [°]
#1 stage	118.596	0.7550	0	227.99	216.59	101.17	19.56
#2 stage	120.4361	0.7667	34.06	274.80	261.06	145.43	21.91

Equation No.	(28)	(29)	(34)	(35)	(36)	(37)	(38)
Parameter	$w_{2s} \left[\frac{m}{s}\right]$	$w_2 \left[\frac{m}{s}\right]$	$v_{2s} \left[\frac{m^3}{kg}\right]$	$v_{1s} \left[\frac{m^3}{kg}\right]$	l_n [m]	l_r [m]	β_2 [°]
#1 stage	125.94	119.64	0.044	0.041	0.0218	0.0229	16.432
#2 stage	171.50	162.92	0.125	0.113	0.0367	0.0379	20.370

Equation No.	(39)	(40)	(43)	(44)	(45)	(46)
Parameter	$c_2 \left[\frac{m}{s}\right]$	α_2 [°]	$a_{1s} \left[\frac{m}{s}\right]$	Ma_{c1s} [–]	$a_{2s} \left[\frac{m}{s}\right]$	Ma_{r2s} [–]
#1 stage	34.063	77.54	192.49	0.5255	194.301	0.61578
#2 stage	65.266	89.99	205.28	0.7123	205.967	0.79421

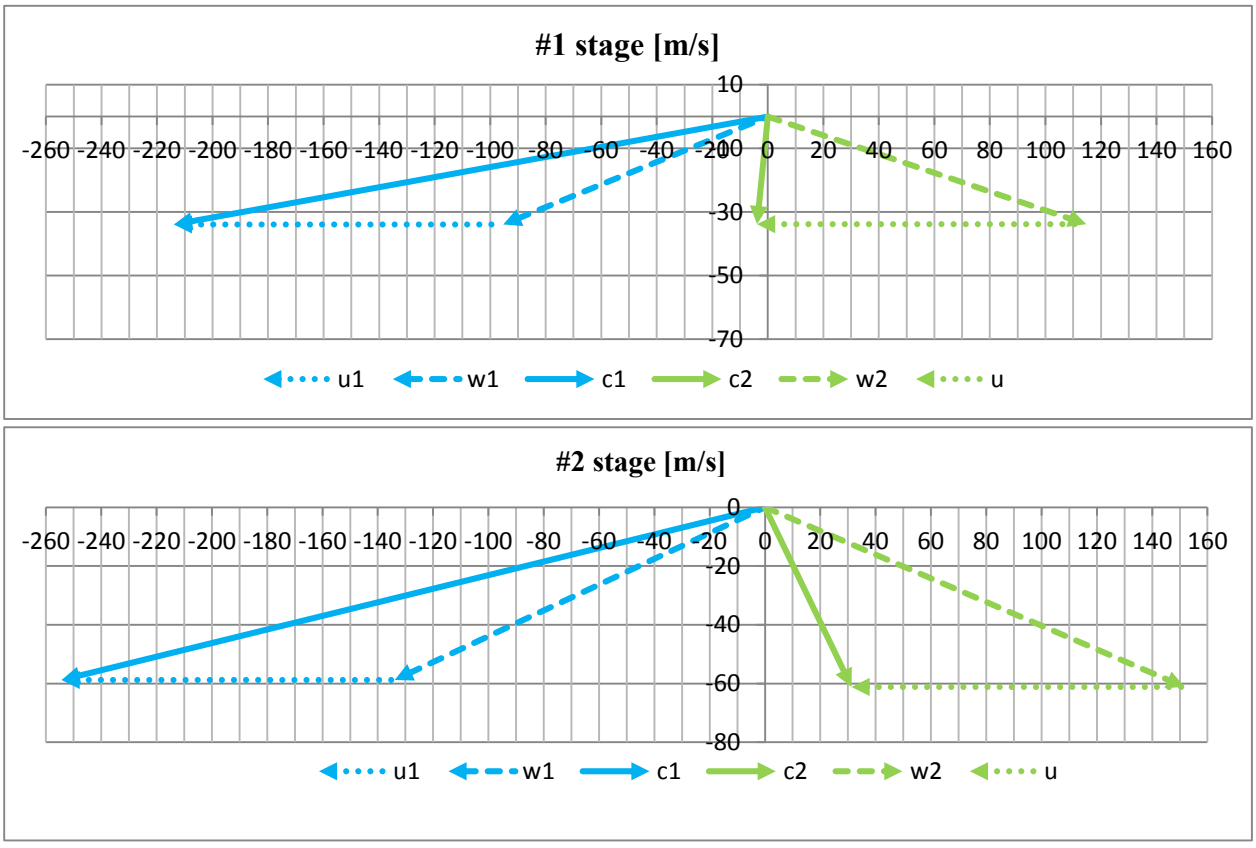

Fig. 7. Velocity triangles of: a) the 1st stage, b) the 2nd stage.

Table 8
Losses, internal efficiencies and internal specific work of turbine stages.

Stage number	$\xi_n[-]$	$\xi_r[-]$	$\xi_f[-]$	$\eta_i[-]$	$l_i[kJ/kg]$
1	0.01868	0.0175	0.0142	0.822	23.414
2	0.01337	0.0095	0.0035	0.795	32.847

$$\eta_{iT} = \frac{\sum l_i}{h_s} = 0.81. \tag{60}$$

3.4. Preliminary geometry of turbine

Additionally, based on the designated nozzle and rotor blade lengths l_n, l_r and average diameter d_{av}, as well as based on standard turbine design guidelines [73,74], an outline design of the two-stage disc type ORC turbine was made, as shown in Fig. 8.

Spiral inlet and spiral outlet is applied. Glands are situated at the shaft in proximity of inlet and outlet. Air traps are situated at the beginning and at the end of casing. Expansions ends at pressure higher than ambient pressure in contrary to conventional steam turbine. Air trap and gland at the end of casing protect from leakage of working fluid, not from air leaking into flowpath. Internal glands are applied at the bottom of second stage stator disc. Interactions between isobutane and elements of turbine is not as well recognized as interactions between water vapour and turbine elements, what could affect characteristics of erosion and aging of used materials. In case of this type of units it is beneficial to apply heat flow diagnostics which could be used to determine potential failures [61,62].

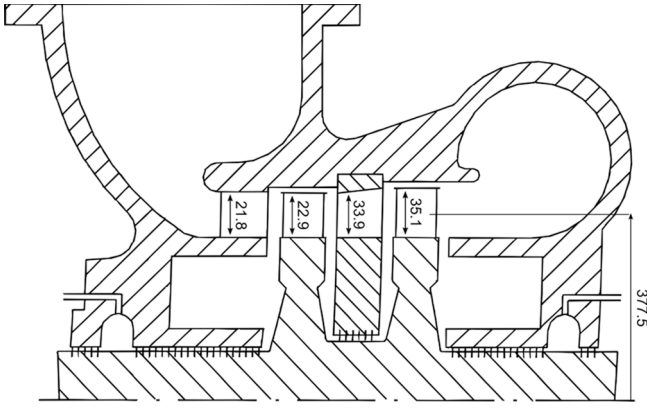

Fig. 8. The outline of a cross-section of the ORC turbine (mm).

4. Scenario for establishing a binary power plant in Poland

The main features of the analysed binary power plant for Polish geothermal conditions are reported in Table 9. Table 10 summarizes the results of calculations for other geothermal power plants that are working at present or have already been dismantled.

Table 9
Main features of binary power plant in Poland ($T_{in} = 120\ ^\circ C$, $T_{out} = 82\ ^\circ C$, $e_{br.in} = 58.93$ kJ/kg, $\dot{V}_{in} = 400\ m^3/h$, $\eta_{iT} = 0.81$, $\eta_{iP} = 0.65$, $\eta_m = 0.98$, $\eta_g = 0.97$).

Parameter	N_e	N_{net}	$\dot{Q}_{in}$	η_I	η_{II}
Unit	kW	kW	kW	%	%
Value	2446	1790	17.348	10.5	29.0

Table 10
Comparison of binary power plants worldwide [68].

City/Province	Country	N_{net} kW	η_I %	η_{II} %	T_{in} °C	T_{out} °C
Brady	USA	4330	8.1	18.3	108	71
Nigorikawa	Japan	1000	9.8	21.6	140	92
Husavik	Iceland	1696	10.6	23.1	127	80
Power plant	**Poland**	**1790**	**10.5**	**29.0**	**120**	**82**
Heber	USA	6875	13.2	43.4	160	–
Otake	Japan	1000	12.9	53.9	130	50

The data in Table 9 indicates that planned binary power plant in Poland could be characterized by 2446 kW_e of power output. From Table 9 it can be also found that the First and the Second Law thermal efficiency are equal to 15,2% and 29.0%, respectively. It should be also noted that the brine temperature at the vaporizer outlet is sufficiently high $T_{out} = 82$ °C, so it is possible brine re-injection without silica scaling but with high exergy (Table 10). Comparing the results of calculations of Polish and worldwide power plants is rather hopeful [68]. From Table 10, it can be seen that for similar geothermal conditions, analysed efficiencies are comparable. For different brine temperature, the First Law thermal efficiency ranges between 12% and 19% and simultaneously, the Second Law thermal efficiency varies between 18% and 54%.

Table 11. presents similar axial turbines that were designed for ORC power plants. Centrifugal turbines are usually preferred for lower powers under 500 kW. For lower powers, axial turbines are not as beneficial because leakage losses are more severe in smaller units. Clearances and thickness of boundary layers contribute to those losses. For higher powers, axial turbines are preferred. Examples of small radial orc turbines for domestic use are described in [59,60]. The analysed turbines designed by different authors did not rotate at rotation speeds synchronous to the power grid, which require transmission and thus, reduces electric power of unit. The turbine designed in this paper rotates at 3000 rpm, which corresponds to the European power grid. Because of lower rotation velocity, this design has higher mean diameter, but did not constitute the construction problem. VR is volumetric expansion ratio and SP is size parameter [58]. These parameters allow comparison of the size of turbines for which bigger units generally have lower losses due to clearances and effects of boundary layers.

5. Conclusions

The comparison between results obtained in this study and those from other studies proves that a binary power plant in Poland can achieve a comparable performance to other worldwide binary power plants (both existing and dismantled). The net power output and the thermal efficiency based on the First Law of Thermodynamics of a binary power plant were estimated at about 2335 kW_e and 15.2%, respectively. All numerical calculations were carried out for the volume flow rate of brine equal to $\dot{V}_{in} = 400$ m^3/h and brine inlet temperature of $T_{in} = 120$ °C. It should be also noted that the brine temperature of $T_{out} = 82$ °C at the vaporizer outlet was sufficiently high; thus, reinjection without silica scaling but with high exergy was possible.

By setting the upper ORC temperature as 97 °C, a preliminary design of the axial action turbine was designed. The resulting efficiency of the turbine at 81% coincided with the cycle assumptions, and the average diameter of the highest stage of 76.6 cm indicated the compact dimensions of the unit. Parameters and dimensions of designed unit were similar to conventional small steam turbines. Because of that finding, construction of such a unit should not be difficult. A designed turbine has relatively cheap construction, which allows a reduction in investment cost and return period.

The average geothermal gradient, brine volume flow rate, and salinity are important parameters that have a crucial impact on both investments cost and reimbursement time, so an economic analysis should be done in next step for a suitable location for a power plant in Poland.

Conducting a combined three-aspect analysis it is ensured that system efficiencies are higher obtained than separately carrying out studies on each of these aspects, which is most clearly demonstrated in Table 10. This table highlights the fact that the complete studies carried out have even achieved higher efficiencies than similar power plants with the same temperatures from the geothermal source or even in one case higher temperatures. The research confirms the validity of the methodology adopted and gives a new result in the literature.

CRediT authorship contribution statement

Paweł Ziółkowski: Conceptualization, Data curation, Formal analysis, Funding acquisition, Investigation, Methodology, Project administration, Resources, Software, Supervision, Validation, Visualization, Writing - original draft. **Rafał Hyrzyński:** Conceptualization, Data curation, Formal analysis, Investigation, Writing - original draft. **Marcin Lemański:** Conceptualization, Data curation, Formal analysis, Investigation, Methodology, Writing - original draft. **Bartosz Kraszewski:** Conceptualization, Data curation, Formal analysis, Investigation, Methodology, Validation, Visualization, Writing - original draft. **Sebastian Bykuć:** Funding acquisition, Software, Writing - review & editing. **Stanisław Głuch:** Data curation, Formal analysis, Investigation, Methodology, Validation, Visualization, Writing - original draft. **Anna Sowiżdżał:** Conceptualization, Data curation, Formal analysis, Funding acquisition, Investigation, Methodology, Project administration, Resources, Software, Supervision, Validation, Visualization, Writing - original draft. **Leszek Pająk:** Conceptualization, Data curation, Formal analysis, Investigation, Methodology, Writing - original draft. **Anna Wachowicz-Pyzik:** Data curation, Formal analysis, Investigation, Software, Writing - review & editing. **Janusz Badur:** Funding acquisition,

Table 11
Comparison of ORC turbines.

Working fluid	N	N_{net}	VR	SP	l_r	d_{av}	r	ω	Publication
Unit	[kW]	[kW]	[–]	[–]	[mm]	[mm]	[–]	[rpm]	–
R600a (isobutane)	2446	1790	6.581	0.7901	35.5	776	0.1	3000	This research
R600a (isobutane)	3980.5	3712.4	4.359	0.1821	–	–	–	9077	[58]
R245fa (1,1,1,3,3-Pentafluoropropane)	3684.9	3570.6	5.061	0.2747	–	–	–	4101	[58]
R236fa (1-Chloro-1,1,3,3,3-pentafluoropropane)	4303.4	3996.3	6.565	0.2373	–	–	–	4067	[58]
R236ea (1,1,1,2,3,3-Hexafluoropropane)	3886.0	3710.8	5.201	0.2583	–	–	–	4009	[58]
MM (hexamethyldisiloxane)	–	300	–	–	57.5	303	0.276	14,500	[76]
R245fa (1,1,1,3,3-Pentafluoropropane)	–	–	1.7	0.22	–	–	0.45	–	[54]
R123 (2,2-Dichloro-1,1,1-trifluoroethane	6.239	–	–	–	16	62	0.5	10000–30000	[57,77]
R134a (1,1,1,2-Tetrafluoroethane)	–	–	–	–	16	62	0.5	10000–30000	[57,77]
R141b (1,1-Dichloro-1-fluoroethane)	–	–	–	–	16	62	0.5	10000–30000	[57,77]
R152a (1,1-Difluoroethane)	–	–	–	–	16	62	0.5	10000–30000	[57,77]
R245fa (1,1,1,3,3-Pentafluoropropane)	–	–	–	–	16	62	0.5	10000–30000	[57,77]
R600a (isobutane)	4.015	–	–	–	16	62	0.5	10000–30000	[57,77]

Software, Writing - review & editing.

Declaration of Competing Interest

The authors declare that they have no known competing financial interests or personal relationships that could have appeared to influence the work reported in this paper.

Acknowledgments

Financial support of these studies from Gdańsk University of Technology by the DEC-50/2020/IDUB/I.3.3 grant under the ARGENTUM TRIGGERING RESEARCH GRANTS – EIRU program is gratefully acknowledged. The part of work has been analysed within the frame of statutory research of the Institute of Fluid Flow Machinery Polish Academy of Sciences. However, the other parts of this paper were performed within the frame of AGH-UST statutory research grant No. 16.16.140.315/05, Faculty of Geology, Geophysics and Environmental Protection, Department of Fossil Fuels.

Appendix A. Supplementary data

Supplementary data to this article can be found online at https://doi.org/10.1016/j.enconman.2021.114672.

References

[1] Hyrzyński R, Karcz M, Lemański M, Lewandowski K, Nojek S. Complementarity of wind and photovoltaic power generation in conditions similar to Polish. Acta Energy 2013;17(4):14–21.
[2] Ziółkowski P, Kowalczyk T, Lemański M, Badur J. On energy, exergy, and environmental aspects of a combined gas-steam cycle for heat and power generation undergoing a process of retrofitting by steam injection. Energy Convers Manag 2019;192:374–84. https://doi.org/10.1016/j.enconman.2019.04.033.
[3] Hyrzyński R, Ziółkowski P, Gotzman S, Kraszewski B, Ochrymiuk T, Badur J. Comprehensive thermodynamic analysis of the CAES system coupled with the underground thermal energy storage taking into account global, central and local level of energy conversion. Renewable Energy 2021;169:379–403. https://doi.org/10.1016/j.renene.2020.12.123.
[4] Badur J, Lemański M, Kowalczyk T, Ziółkowski P, Kornet S. Zero-dimensional robust model of an SOFC with internal reforming for hybrid energy cycles. Energy 2018;158:128–38. https://doi.org/10.1016/j.energy.2018.05.203.
[5] DiPippo R. Geothermal power plants. Elsevier 2008. https://doi.org/10.1016/B978-0-7506-8620-4.X5001-1.
[6] Kantorek M, Jesionek K, Polesek-Karczewska S, Ziółkowski P, Stajnke M, Badur J. Thermal utilization of meat-and-bone meal using the rotary kiln pyrolyzer and the fluidized bed boiler – The performance of pilot-scale installation. Renewable Energy 2021;164:1447–56. https://doi.org/10.1016/j.renene.2020.10.124.
[7] Wachowicz-Pyzik A, Sowiżdżał A, Pająk L, Ziółkowski P, Badur J. Assessment of the effective variants leading to higher efficiency for the geothermal doublet, using numerical analysis-case study from Poland (Szczecin trough). Energies 2020;13(9):2174. https://doi.org/10.3390/en13092174.
[8] European Council. European Council (23 and 24 October 2014) Conclusions on 2030 Climate and Energy Policy Framework; 2014.
[9] Cataldi. The centenary of the geothermal - electric industry: historical outline, celebration program, and outcome. Exploration Technology Geothermal Energy. Sustainable Dev 2006;1.
[10] Huttrer GW. Geothermal Power Generation in the World 2015–2020 Update Report. Proc World Geotherm Congr 2020;2020:1–17.
[11] DiPippo R. Geothermal power plants: Evolution and performance assessments. Geothermics 2015;53:291–307. https://doi.org/10.1016/j.geothermics.2014.07.005.
[12] Tomasini-Montenegro C, Santoyo-Castelazo E, Gujba H, Romero RJ, Santoyo E. Life cycle assessment of geothermal power generation technologies: an updated review. Appl Therm Eng 2017;114:1119–36. https://doi.org/10.1016/j.applthermaleng.2016.10.074.
[13] Loloum T, Abram S, Ortar N. Ethnographies of Power: A Political Anthropology of. Energy. 2021.
[14] Reuters Staff. Poland to close coal mines by 2049 in deal with unions; 2020.
[15] Madhawa Hettiarachchi HD, Golubovic M, Worek WM, Ikegami Y. Optimum design criteria for an Organic Rankine cycle using low-temperature geothermal heat sources. Energy 2007;32(9):1698–706. https://doi.org/10.1016/j.energy.2007.01.005.
[16] Kaczmarczyk M, Tomaszewska B, Pająk L. Geological and thermodynamic analysis of low enthalpy geothermal resources to electricity generation using ORC and Kalina Cycle Technology. Energies 2020;13:1335. https://doi.org/10.3390/en13061335.
[17] Barbacki A, Pająk L. Assessment of possibilities of electricity production in flash geothermal system in Poland. Geomatics Environ Eng 2017;11(3):17. https://doi.org/10.7494/geom.2017.11.3.17.
[18] Bujakowski W, Tomaszewska B, editors. Atlas of the possible use of geothermal waters for combined production of electricity and heat using binary systems in Poland. Kraków, Poland: Polish Academy of Sciences; 2014 (in Polish).
[19] Stanek W, Gazda W, Kostowski W. Thermo-ecological assessment of CCHP (combined cold-heat-and-power) plant supported with renewable energy. Energy 2015;92:279–89. https://doi.org/10.1016/j.energy.2015.02.005.
[20] Sowiżdżał A. Geothermal energy resources in Poland – overview of the current state of knowledge. Renewable Sustainable Energy Rev 2018;82:4020–7. https://doi.org/10.1016/j.rser.2017.10.070.
[21] Kępińska B. Geothermal Energy Use - Country Update for Poland, 2016-2018. Eur. Geotherm. Congr. 11-14 June, Den Haag, The Netherlands; 2019.
[22] Sowiżdżał A, Górecki W, Hajto M. Geological conditions of geothermal resource occurrences in Poland. Geol Q 2020;64:185–96. https://doi.org/10.7306/gq.1526.
[23] Sowiżdżał A, Papiernik B, Machowski G, Hajto M. Characterization of petrophysical parameters of the lower triassic deposits in a prospective location for enhanced geothermal system (central Poland). Geol Q 2013;57:729–44. https://doi.org/10.7306/gq.1121.
[24] Wójcicki A, Sowiżdżał A, Bujakowski W. Evaluation of potential, thermal balance and prospective geological structures for needs of closed geothermal systems. Warszawa/Kraków: Ministerstwo Środowiska; 2013 (in Polish).
[25] Anderson A, Rezaie B. Geothermal technology: trends and potential role in a sustainable future. Appl Energy 2019;248:18–34. https://doi.org/10.1016/j.apenergy.2019.04.102.
[26] Tester JW, Anderson BJ, Batchelor AS, Blackwell DD, DiPippo R, Drake EM, et al. Impact of enhanced geothermal systems on US energy supply in the twenty-first century. Philos Trans R Soc A Math Phys Eng Sci 2007;365(1853):1057–94. https://doi.org/10.1098/rsta.2006.1964.
[27] Gorecki W, Szczepański J, Sadurski A, Hajto M, Papiernik B, Szewczyk J, et al. Atlas of Geothermal resources of mesozoic formations in the Polish Lowlands. Kraków, Poland: AGH University of Science and Technology; 2006.
[28] Górecki W, Sowiżdżał A, Hajto M, Wachowicz-Pyzik A. Atlases of geothermal waters and energy resources in Poland. Environ Earth Sci 2015;74(12):7487–95. https://doi.org/10.1007/s12665-014-3832-2.
[29] Sowiżdżał A, Tomaszewska B, Chmielowska A. Development of the Polish geothermal sector in the light of current possibilities of financial support for a geothermal investment. E3S Web Conf 2019;86:34. https://doi.org/10.1051/e3sconf/20198600034.
[30] Portal Gospodarczy n.d. <https://www.wnp.pl/> [accessed October 8, 2020].
[31] Gładysz P, Sowiżdżał A, Miecznik M, Hacaga M, Pająk L. Techno-economic assessment of a combined heat and power plant integrated with carbon dioxide removal technology: a case study for central Poland. Energies 2020;13(11):2841. https://doi.org/10.3390/en13112841.
[32] Blaise M, Feidt M, Maillet D. Influence of the working fluid properties on optimized power of an irreversible finite dimensions Carnot engine. Energy Convers Manag 2018;163:444–56. https://doi.org/10.1016/j.enconman.2018.02.056.
[33] Desideri U, Bidini G. Study of possible optimisation criteria for geothermal power plants. Energy Convers Manag 1997;38(15-17):1681–91. https://doi.org/10.1016/S0196-8904(96)00209-9.
[34] Ziółkowski P, Kowalczyk T, Kornet S, Badur J. On low-grade waste heat utilization from a supercritical steam power plant using an ORC-bottoming cycle coupled with two sources of heat. Energy Convers Manag 2017;146:158–73. https://doi.org/10.1016/j.enconman.2017.05.028.
[35] Mikielewicz D, Wajs J, Ziółkowski P, Mikielewicz J. Utilisation of waste heat from the power plant by use of the ORC aided with bleed steam and extra source of heat. Energy 2016;97:11–9. https://doi.org/10.1016/j.energy.2015.12.106.
[36] Kowalczyk T, Badur J, Ziółkowski P. Comparative study of a bottoming SRC and ORC for Joule-Brayton cycle cooling modular HTR exergy losses, fluid-flow machinery main dimensions, and partial loads. Energy 2020;206:118072. https://doi.org/10.1016/j.energy.2020.118072.
[37] Ziółkowski P, Hernet J, Badur J. Revalorization of the Szewalski binary vapour cycle. Arch Thermodyn 2014;35:225–49.
[38] Hung TC, Shai TY, Wang SK. A review of organic rankine cycles (ORCs) for the recovery of low-grade waste heat. Energy 1997;22(7):661–7. https://doi.org/10.1016/S0360-5442(96)00165-X.
[39] Gnutek Z, Bryszewska-Mazurek A. The thermodynamic analysis of multicycle ORC engine. Energy 2001;26(12):1075–82. https://doi.org/10.1016/S0360-5442(01)00070-6.
[40] Wei D, Lu X, Lu Z, Gu J. Performance analysis and optimization of organic Rankine cycle (ORC) for waste heat recovery. Energy Convers Manag 2007;48(4):1113–9. https://doi.org/10.1016/j.enconman.2006.10.020.
[41] Borsukiewicz - Gozdur A, Nowak W. Comparative analysis of natural and synthetic refrigerants in application to low temperature Clausius-Rankine cycle. Energy 2007;32(4):344–52. https://doi.org/10.1016/j.energy.2006.07.012.
[42] Wang XD, Zhao L. Analysis of zeotropic mixtures used in low-temperature solar Rankine cycles for power generation. Sol Energy 2009;83(5):605–13. https://doi.org/10.1016/j.solener.2008.10.006.
[43] Moya P, DiPippo R. Unit 5 bottoming binary plant at Miravalles geothermal field, Costa Rica: Planning, design, performance and impact. Geothermics 2007;36(1):63–96. https://doi.org/10.1016/j.geothermics.2006.10.003.
[44] Walraven D, Laenen B, D'haeseleer W. Comparison of thermodynamic cycles for power production from low-temperature geothermal heat sources. Energy Convers Manag 2013;66:220–33. https://doi.org/10.1016/j.enconman.2012.10.003.

[45] Ghasemi H, Paci M, Tizzanini A, Mitsos A. Modeling and optimization of a binary geothermal power plant. Energy 2013;50:412–28. https://doi.org/10.1016/j.energy.2012.10.039.
[46] Witanowski Ł, Klonowicz P, Lampart P, Suchocki T, Jędrzejewski Ł, Zaniewski D, et al. Optimization of an axial turbine for a small scale ORC waste heat recovery system. Energy 2020;205:118059. https://doi.org/10.1016/j.energy.2020.118059.
[47] Dong B, Xu G, Luo X, Zhuang L, Quan Y. Analysis of the supercritical organic Rankine cycle and the radial turbine design for high temperature applications. Appl Therm Eng 2017;123:1523–30. https://doi.org/10.1016/j.applthermaleng.2016.12.123.
[48] Fiaschi D, Manfrida G, Maraschiello F. Design and performance prediction of radial ORC turboexpanders. Appl Energy 2015;138:517–32. https://doi.org/10.1016/j.apenergy.2014.10.052.
[49] Fiaschi D, Innocenti G, Manfrida G, Maraschiello F. Design of micro radial turboexpanders for ORC power cycles: From 0D to 3D. Appl Therm Eng 2016;99:402–10. https://doi.org/10.1016/j.applthermaleng.2015.11.087.
[50] Da Lio L, Manente G, Lazzaretto A. Predicting the optimum design of single stage axial expanders in ORC systems: Is there a single efficiency map for different working fluids? Appl Energy 2016;167:44–58. https://doi.org/10.1016/j.apenergy.2016.01.020.
[51] Khalil KM, Mahmoud S, Al-Dadah RK. Development of innovative non-repeated annular area dual stage small-scale nitrogen axial turbine for hybrid open-closed Rankine cycle. Energy Convers Manag 2018;164:157–74. https://doi.org/10.1016/j.enconman.2018.02.088.
[52] Maral H, Alpman E, Kavurmacıoğlu L, Camci C. A genetic algorithm based aerothermal optimization of tip carving for an axial turbine blade. Int J Heat Mass Transfer 2019;143:118419. https://doi.org/10.1016/j.ijheatmasstransfer.2019.07.069.
[53] Martins GL, Braga SL, Ferreira SB. Design optimization of partial admission axial turbine for ORC service. Appl Therm Eng 2016;96:18–25. https://doi.org/10.1016/j.applthermaleng.2015.09.041.
[54] Talluri L, Lombardi G. Simulation and Design Tool for ORC Axial Turbine Stage. Energy Procedia 2017;129:277–84. https://doi.org/10.1016/j.egypro.2017.09.154.
[55] Meroni A, Andreasen JG, Persico G, Haglind F. Optimization of organic Rankine cycle power systems considering multistage axial turbine design. Appl Energy 2018;209:339–54. https://doi.org/10.1016/j.apenergy.2017.09.068.
[56] Touil K, Ghenaiet A. Characterization of vane - blade interactions in two-stage axial turbine. Energy 2019;172:1291–311.
[57] Al Jubori AM, Al-Dadah R, Mahmoud S. An innovative small-scale two-stage axial turbine for low-temperature organic Rankine cycle. Energy Convers Manag 2017;144:18–33. https://doi.org/10.1016/j.enconman.2017.04.039.
[58] Lazzaretto A, Manente G. A new criterion to optimize ORC design performance using efficiency correlations for axial and radial turbines. Int J Thermodyn 2014;17:173–81. https://doi.org/10.5541/ijot.562.
[59] Kaczmarczyk TZ, Żywica G, Ihnatowicz E. The impact of changes in the geometry of a radial microturbine stage on the efficiency of the micro CHP plant based on ORC. Energy 2017;137:530–43. https://doi.org/10.1016/j.energy.2017.05.166.
[60] Kaczmarczyk TZ, Żywica G, Ihnatowicz E. Experimental study of a low-temperature micro-scale organic Rankine cycle system with the multi-stage radial-flow turbine for domestic applications. Energy Convers Manag 2019;199:111941. https://doi.org/10.1016/j.enconman.2019.111941.
[61] Głuch J, Krzyżanowski J. New Attempt for Diagnostics of the Geometry Deterioration of the Power System Based on Thermal Measurement. Vol. 2 Aircr. Engine; Ceram. Coal, Biomass Altern. Fuels; Control. Diagnostics Instrumentation; Environ. Regul. Aff., ASMEDC; 2006, p. 531–9. https://doi.org/10.1115/GT2006-90263.
[62] Butterweck A, Głuch J. Neural network simulator's application to reference performance determination of turbine blading in the heat-flow diagnostics. Power Syst 2014;28:137–47. https://doi.org/10.1007/978-3-642-39881-0_11.
[63] Klonowicz P, Witanowski Ł, Suchocki T, Jędrzejewski Ł, Lampart P. Selection of optimum degree of partial admission in a laboratory organic vapour microturbine. Energy Convers Manag 2019;202:112189. https://doi.org/10.1016/j.enconman.2019.112189.
[64] Cavazzini G, Dal Toso P. Techno-economic feasibility study of the integration of a commercial small-scale ORC in a real case study. Energy Convers Manag 2015;99:161–75. https://doi.org/10.1016/j.enconman.2015.04.043.
[65] Yamamoto T, Furuhata T, Arai N, Mori K. Design and testing of the Organic Rankine Cycle. Energy 2001;26(3):239–51. https://doi.org/10.1016/S0360-5442(00)00063-3.
[66] Kotas TJ. Exergy analysis of simple processes. Exergy Method Therm Plant Anal 1985:99–161. https://doi.org/10.1016/b978-0-408-01350-5.50011-8.
[67] Szargut J, Morris D, Steward F. Exergy analysis of thermal, chemical, and metallurgical processes. Hemisphere Publishing Corporation; 1988.
[68] DiPippo R. Second Law assessment of binary plants generating power from low-temperature geothermal fluids. Geothermics 2004;33(5):565–86. https://doi.org/10.1016/j.geothermics.2003.10.003.
[69] Dağdaş A, Öztürk R, Bekdemir Ş. Thermodynamic evaluation of Denizli Kızıldere geothermal power plant and its performance improvement. Energy Convers Manag 2005;46(2):245–56. https://doi.org/10.1016/j.enconman.2004.02.021.
[70] Zare V. A comparative exergoeconomic analysis of different ORC configurations for binary geothermal power plants. Energy Convers Manag 2015;105:127–38. https://doi.org/10.1016/j.enconman.2015.07.073.
[71] Kowalczyk T, Ziółkowski P, Badur J. Exergy losses in the Szewalski binary vapor cycle. Entropy 2015;17:7242–65. https://doi.org/10.3390/e17107242.
[72] Ziółkowski P, Mikielewicz D, Mikielewicz J. Increase of power and efficiency of the 900 MW supercritical power plant through incorporation of the ORC. Archives of Thermodynamics 2013;34(4):51–71. https://doi.org/10.2478/aoter-2013-0029.
[73] Perycz S. Steam and gas turbines (in Polish). Gdańsk University of Technology; 1988.
[74] Kosowski K, editor. Steam and gas turbines with examples of Alstom technology. Elbląg, Poland: ALSTOM Power; 2007.
[75] National Institute of Standards and Technology. NIST-Chemistry Webbook - Thermophysical Properties of Fluid Systems n.d. <https://webbook.nist.gov/chemistry/fluid/> [accessed February 11, 2019].
[76] Zaniewski D, Klimaszewski P, Witanowski Ł, Jędrzejewski Ł, Klonowicz P, Lampart P. Comparison of an impulse and a reaction turbine stage for an ORC power plant. Arch Thermodyn 2019;40:137–57. https://doi.org/10.24425/ather.2019.129998.
[77] Al Jubori A, Al-Dadah RK, Mahmoud S, Bahr Ennil AS, Rahbar K. Three dimensional optimization of small-scale axial turbine for low temperature heat source driven organic Rankine cycle. Energy Convers Manag 2017;133:411–26. https://doi.org/10.1016/j.enconman.2016.10.060.